

# AMBER – physics simulations for a new experiment at CERN

Rita Ataíde da Silva<sup>1,a</sup>

<sup>1</sup>Instituto Superior Técnico, Lisboa, Portugal

Project supervisor: C. Quintans

October 2019

**Abstract.** AMBER is a new project for a fixed target experiment at CERN. One of its goals is to learn about quarks and gluons dynamics inside hadrons. Physics simulations were performed using Pythia8 in order to analyze a very rare process, Drell-Yan. Drell-Yan is a quark-antiquark annihilation, where the resulting virtual photon decays to a pair of muons. The starting point was to study all the accompanying particles produced, and then focus on the kinematic variables associated to the dimuon, from the transverse momentum to the fraction of hadron momentum carried by the struck quark, Bjorken- $x$ . The acceptance of the detector was also simulated, by applying some cuts to the muons polar angle. Finally, it was analyzed the effects of proton misidentification by a pion.

KEYWORDS: AMBER, PYTHIA, Bjorken  $x$

## 1 Introduction

### 1.1 AMBER

The COMPASS++/AMBER (proto-) collaboration proposes to establish a “New QCD facility at the M2 beam line of the CERN SPS”. It will allow a great variety of measurements to address fundamental issues of Quantum Chromodynamics. [1]

A beam made of hadrons, with 190 GeV/c will collide with a target. It is possible to have a positive or a negative hadron beam. The former is composed of  $\pi^+$ , protons and  $K^+$  and the latter of their antiparticles.

Before the target, there will be two CEDAR detectors that are able to identify the beam particle type. The target will consist of three cylinders made of carbon.

After that, there will be a hadron absorber in order to absorb the hadrons produced in the interaction with the target, since the main goal is to detect the muons.

Continuing downstream, there will be many tracking detectors, including a muon filter, where the muons are detected.

In between the detectors mentioned there is a dipole magnet (per spectrometer stage), which is used to measure the charged particles momentum, from their measured bending angle when crossing the magnetic field.

### 1.2 Relevant variables

Here we present a list of the main variables which will be measured with the detector and were simulated in this analysis.

For the muons:

- $\theta$  : polar angle of the trajectory of a particle with respect to the pion beam trajectory;
- $\phi$  : azimuthal angle of the trajectory of the particle, measured in the plane transverse to the direction of the pion beam;

For the dimuon:

- $p_T$  : transverse momentum;
- $p_{Abs}$  : absolute momentum;
- $M$  : invariant mass;

### 1.3 The Drell-Yan Process

Drell-Yan (DY) is a very rare process, which takes place when a quark of one hadron and an antiquark of another hadron annihilate, creating a virtual photon, which then decays into a pair of oppositely-charged muons.

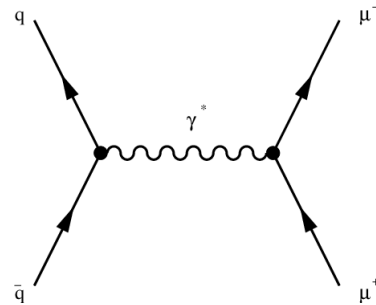


Figure 1. Feynman diagram for DY

It provides valuable information about the parton distribution functions (PDF's) of the colliding hadrons, which are essential for calculating physics processes initiated by them. The PDF's describe the way the momentum of a hadron is partitioned among its constituent partons.

Throughout the work done, the Drell-Yan process was simulated only at Leading Order in QCD, that is considering only the Feynman graph from Fig. 1. This is the simplest and purely electromagnetic contribution to DY, without even the possibility for initial or final state radiation.

<sup>a</sup>e-mail: rita.ataide.silva@tecnico.ulisboa.pt

## 2 Simulations using PYTHIA and ROOT

PYTHIA is a program that allows to simulate high-energy physics events using Monte-Carlo methods.

It contains theory and models for various physics processes, including parton distributions, initial and final state parton showers and hard and soft interactions. In this analysis the version 8.2.35 from PYTHIA was used.

In order to simulate Drell-Yan, there were several PYTHIA options used, included in table 1.

**Table 1.** Criteria for event selection in PYTHIA

Variable	
WeakSingleBoson: ffbar2gmZ	on
Beams:	
idA	(+/-)211
idB	2212 / 2112
frameType	3
pxA	0
pyA	0
pzA	190
pxB	0
pyB	0
pzB	0
BeamRemnants:	
primordialKT	on
primordialKTsoft	1.1
primordialKTthard	1.8
halfScaleForKT	2.0
halfMassForKT	4.0
primordialKTremnant	0.4
PhaseSpace: pTHatMinDiverge	
PartonLevel: FSR	off
PartonLevel: ISR	off
23:	
OnMode	off
onIfall	13 -13
mMin	4
mMax	9

In the simulation of the DY interaction, a beam pion (particle A), with longitudinal momentum equal to 190 GeV/c, collides with a target particle (particle B), a proton or a neutron at rest. Since carbon is an isoscalar element, it contains the same amount of protons and neutrons, so both type of collisions are analysed in this simulation.

As mentioned in the previous section, the purpose of this project was only to study DY Leading Order, so initial- and final-state radiation were turned off.

In DY, the quark and anti-quark can annihilate each other and produce a Z boson or a photon. Despite that, at the energy of the simulated collisions, only the DY mediated by  $\gamma^*$  is occurring.

The mass of the dimuon produced was limited in the simulation, to be 4 to 9 GeV/c<sup>2</sup>, since this is the invariant mass

range where experimentally other competing physics processes can be neglected, as shown in Fig. 2.

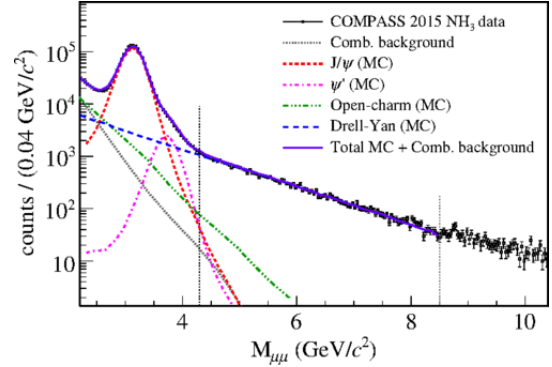


**Figure 2.** The dimuon invariant mass distribution from Ref.[2]

The distribution was made using COMPASS data from pion induced collisions. Since AMBER will be a fixed target experiment using the same beam line, and parts of that same spectrometer, it will be similar to COMPASS in many aspects.

All the simulations and plots made used 200000 events, in order to have a considerable sample and avoid fluctuations.

## 3 Simulation Results

### 3.1 Cross Section

In particle physics, a cross section describes the likelihood of two particles interacting under certain conditions. In this case, it evaluates how frequent is the DY process under different targets and beams.

**Table 2.** PYTHIA Drell-Yan cross sections in LO, for the dimuon mass range  $4 < M_{\mu\mu} / (\text{GeV}/c^2) < 9$

beam and target	$\sigma_{LO}^{DY}$ (nb)
$\pi^-$ p	0.1460
$\pi^-$ n	0.07531
$\pi^+$ p	0.03494
$\pi^+$ n	0.05141

As presented in table 2, it is possible to verify that the cross section of the interaction of a  $\pi^-$  with a proton is the double of the one with a neutron. Which makes sense, since there are two valence quarks up in a proton and only one in the neutron. Therefore, there is twice the probability of having DY in that interaction, since the  $\pi^-$  quarks are  $\bar{u}d$ .

From this type of valence quark species considerations, one could expect that the cross section of  $\pi^+$ -n would be larger than the one of  $\pi^-$ -n. But in fact this is not the case, as confirmed by table 2, since the Drell-Yan cross section goes up proportionally to the square of the annihilating quarks charge, see equation (3.8) presented in

Ref.[3], and a u-quark has a charge of  $+2/3$  while a d-quark has charge  $-1/3$ .

It is important to note that the experimental cross section measured is larger by a factor of two with respect to DY Leading Order one. This also allows to conclude that Next to Leading order, next to next leading order, and so on, all summed up, they contribute as much as DY Leading order.

### 3.2 The Final State Particles

Although the simulation was restricted to the decay channel into muons, there are a lot of other particles produced by the accompanying quarks of the DY process. Analysing which particles, from all the ones produced, are final state, allows to organize them in the table 3. This table corresponds to the DY interaction of a  $\pi^+$  beam with a proton at rest. Nevertheless, the  $\pi^+/\pi^-$  induced DY lead to very similar final state abundances.

**Table 3.** Abundances of the Final State Particles for  $\pi^+ - p$

$\gamma$	41.7 %
$\pi^-$	14.1 %
$\pi^+$	20.7 %
p	4.4 %
n	2.5 %

It was studied the absolute momenta of these particles produced, which are shown in Fig. 3.

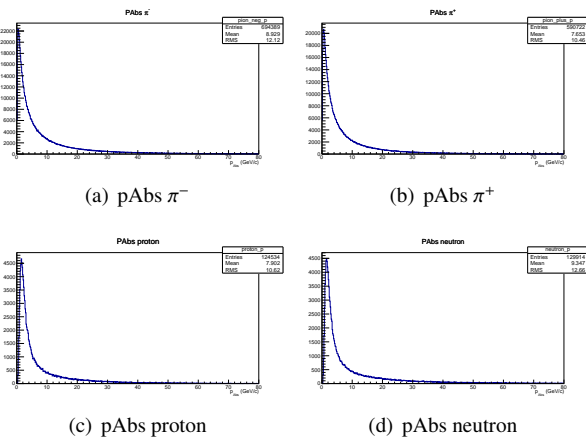


**Figure 3.** Absolute Momentum of the Resulting Particles

The average absolute momentum for these particles is between 7.6 and 8.5 GeV/c and less than 10% of the particles in each case have a momentum higher than 20 GeV/c.

In Fig. 4, the absolute momentum of the muons resulting from the DY process is presented. The corresponding mean value is  $\langle p_{Abs} \rangle = 36.61$  GeV/c. This confirms that, in fact, all the other particles produced are softer than the muons, which result from a hard partonic process.

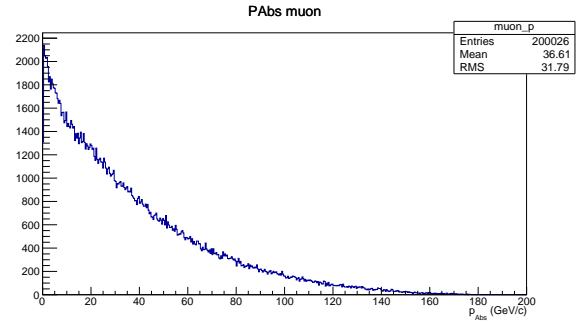


**Figure 4.** Muon Absolute Momentum

### 3.3 Dimuon Produced

Since the muons are the products from the DY process, it is important to study their relevant features, in order to optimise the detectors and the trigger system.

Using PYTHIA, it is easy to obtain the dimuon kinematic variables, from the muon and anti-muon four-vectors.

Fig. 5(a) shows the plot of the invariant mass of the Dimuon. Comparing to the Fig. 2, it is possible to verify, that in fact we are only simulating the region where DY dominates.

One feature of this process is the mean value for the dimuon  $p_T$  around 1 GeV/c, as can be verified for this simulation in Fig. 5(b). The corresponding mean value obtained was  $\langle p_T \rangle = 1.053$  GeV/c.

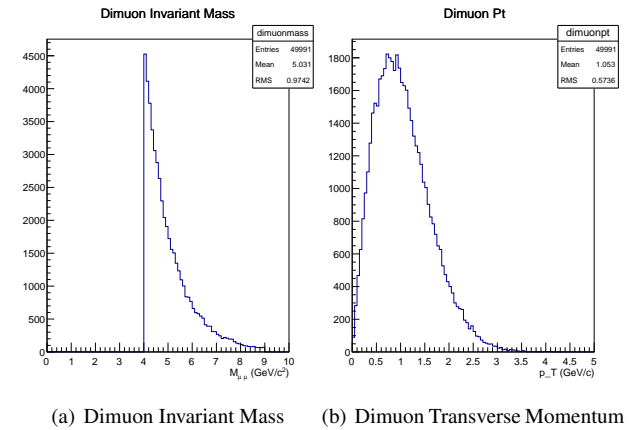


**Figure 5.** Features of the Dimuon produced for the interaction  $\pi^+ - p$

### 3.4 Proton Misidentification

#### 3.4.1 Beam Composition

As mentioned in section 1.1, the charged hadron beams are a mix of long-lived hadrons, so there won't be only pions, but also kaons and protons. There is a different hadron composition of positive and negative beams, as presented in Fig.6.

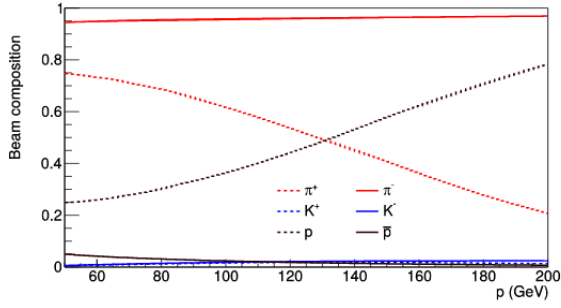


**Figure 6.** The composition of the hadron beam for different energies from Ref. [1].

At the energy of the beam for this experiment (190 GeV), there would be no problem associated with the negative hadron beam, since the  $\pi^-$  constitute around 96% of all the negative particles in the beam, so the error associated with choosing other negative charged hadron can be considered a negligible systematic error. On the other hand, the  $\pi^+$  constitute only 25% of all the positive hadron beam, where the protons contribute with almost 75%. Considering that one of the main goals of AMBER is to study the structure of the pions, it is crucial to identify the DY events induced by pions. As mentioned in section 1.1, the CEDARs are used for the identification of the beam particle that is interacting. Nevertheless, since the CEDARs efficiency is not 100%, the situation where a proton colliding with the target is misidentified as a pion colliding with the target was simulated. This allows to analyze if in fact it will change notoriously the DY kinematic variables.

### 3.4.2 Bjorken $x$

The Bjorken  $x$  corresponds to the fraction of momentum of a quark with respect to its hadron parent. To calculate it, we use the equation (1), presented in Ref. [1].

$$x_{\pi(N)} = \frac{q^2}{2P_{\pi(N)} \cdot q} \quad (1)$$

where  $q^2 = M_{\mu\mu}^2$ , the invariant mass squared of the dimuon,  $P_{\pi(N)}$  is the four-vector momentum of the beam (target) hadron and  $q$  is the four-vector momentum of the virtual photon or equivalently the sum of the four-momentum of the two muons.

Using PYTHIA, one can easily obtain the pion and nucleon Bjorken  $x$  of each DY event.

For the beam, the effects of misidentifying a proton as a pion are illustrated in Fig. 7(a).

It shows that for lower values of this variable, the curve for the proton misidentified as pion (red) and the one identified as a proton (blue) are almost coincident. For values higher than 0.5 they begin to differ. Fig. 7(b) studies how they differ from each other, where the value for the Bjorken  $x$  of the pion misidentified is divided by the proton correctly identified.

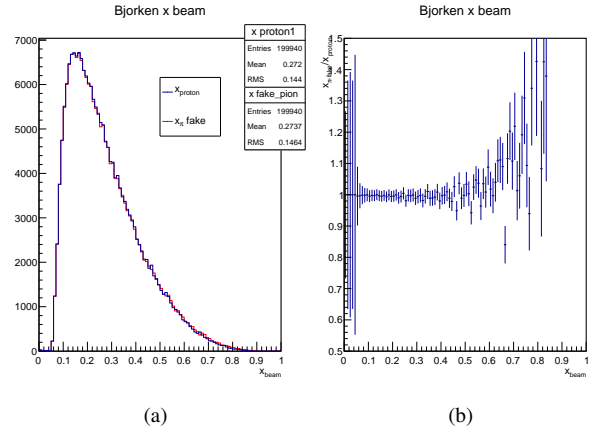


**Figure 7.** Bjorken  $x$  of the beam particle. Blue: correctly identified beam particle; red: misidentified beam particle. The right-hand side plot corresponds to the ratio between the distributions with the misidentified beam particle and with the correctly identified beam.

The impact of beam misidentification becomes relevant at large  $x_\pi$ , reaching up to 40% effect in the assumption of total misidentification.

The same procedure was followed for the target Bjorken  $x$ ,  $x_N$ . It is important to notice that the beam misidentification has no impact in this variable.

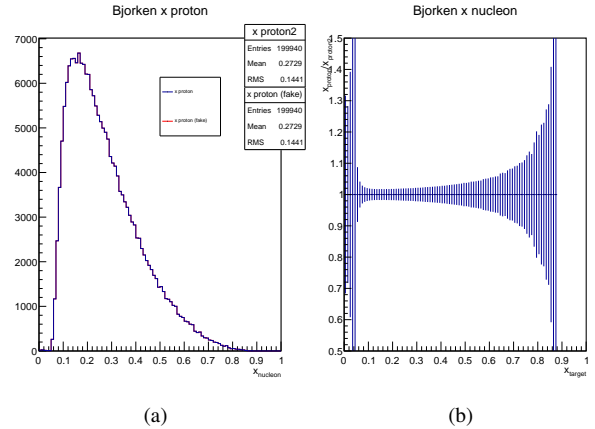


**Figure 8.** Bjorken  $x$  of the target particle. Blue: correctly identified beam particle; red: misidentified beam particle. The right-hand side plot corresponds to the ratio between the distributions with the target proton from the misidentified case and with the right one.

### 3.4.3 Feynman $x$

The Feynman  $x$  relates the Bjorken  $x$  of the beam particle with the one from the target particle. Using the equation 2, presented in Ref. [1], one is able to calculate it.

$$x_F = x_\pi - x_N \quad (2)$$

Note that, since the plots from the target particle, shown in Fig.8(a), are overlaid, the differences in  $x_F$  will come solely from the beam Bjorken  $x$  in each case.

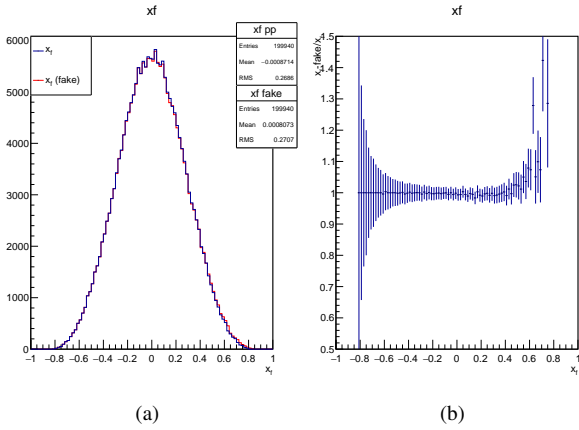


**Figure 9.** Feynman  $x$  distribution. Blue: correctly identified beam particle; red: misidentified beam particle. The right-hand side plot corresponds to the ratio between the misidentified Feynman  $x$  and the one which is correctly identified.

As the plot in Fig. 7(a) shows, the two curves of the plot in Fig. 9(a) differ for higher values of  $x_F$ . This is more visible in 9(b), where the ratio begins to grow almost exponentially for  $x_F$  higher than 0.6.

### 3.5 Detectors Acceptance

As mentioned before, the beam that interacts with the fixed target, has solely longitudinal momentum. Therefore, the sum of transverse momenta of all produced particles taken together is expected to be zero. Given the large momentum of the beam, the produced particles are also expected to be emitted in the forward direction, at relatively low polar angle  $\theta$ .

Fig. 10 shows the polar angle distribution for the muons.

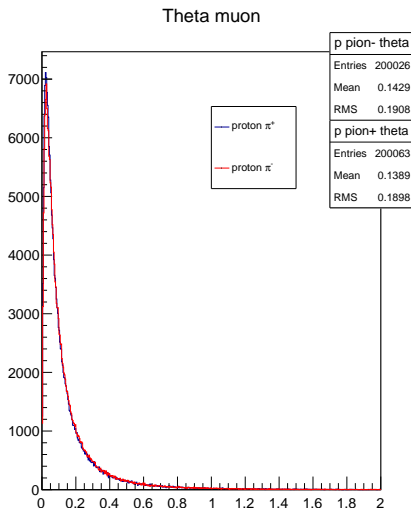


**Figure 10.** Muon theta distribution. Blue  $\pi^+$ -p ; red:  $\pi^-$ -p

In order to simulate the real experiment conditions, some cuts were applied on  $\theta$ . The polar angle cuts that reflect the COMPASS acceptance [4] were:

- Both muons with  $25 \text{ mrad} < \theta_\mu < 160 \text{ mrad}$ ;

OR

- One with  $25 \text{ mrad} < \theta_\mu < 160 \text{ mrad}$  and the other with  $8 \text{ mrad} < \theta_\mu < 45 \text{ mrad}$ .

These angles allowed an acceptance of 49%, which is higher than the COMPASS one, since using PYTHIA we are simulating a single point collision, what differs from the real experiment with an extended target. In AMBER the goal is to obtain, at least, the same acceptance as COMPASS.

The acceptance is defined as the ratio between the number of events where both muons are within the detection range of the spectrometer detectors to the total number of generated events and it can be shown as a function of different Drell-Yan kinematic variables.

The following simulations were made using a beam made of  $\pi^+$  and colliding it with a proton.

#### 3.5.1 Dimuon Transverse Momentum

The dimuon  $p_T$  distribution before and after applying the angular cuts are shown in Fig. 11. Although in Fig. 11(a) the two curves have apparently the same shape, the ratio plot in Fig. 11(b) shows that this is not exactly the case. This plot is the so-called geometrical acceptance as function of  $p_T$  which is seen to slowly decrease as the dimuon  $p_T$  increases.

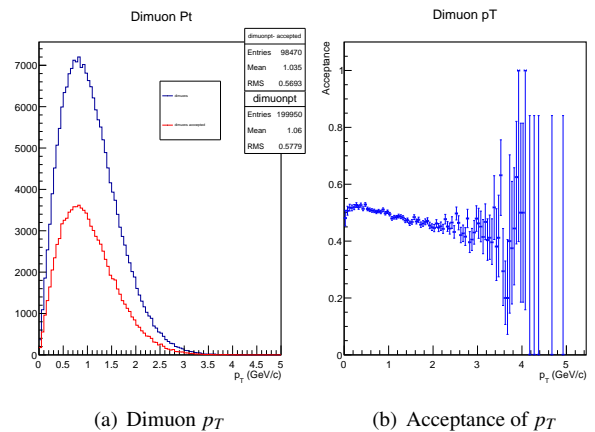


**Figure 11.** Dimuon Transverse Momentum distribution. Blue: the total of events; red: accepted events. Right-hand side: the geometrical acceptance as function of  $p_T$ .

#### 3.5.2 Bjorken $x$

To evaluate how the angular selection made affects the beam Bjorken  $x$  distribution of events, Fig. 12 is shown.

On a first examination, it is immediately visible that each curve in Fig. 12(a) do not peak at the same value. The lower values of  $x_\pi$  are not accepted by the angular cuts applied.

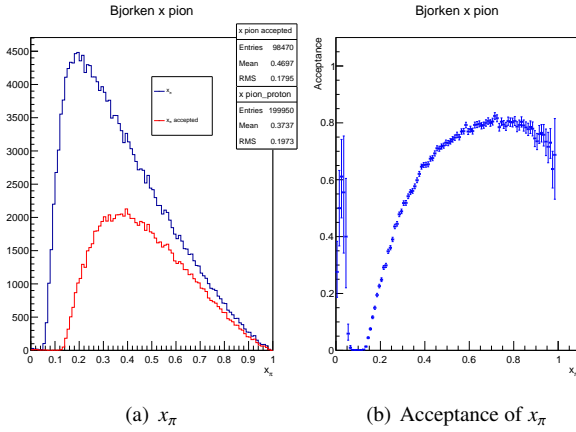


**Figure 12.** The pion Bjorken  $x$ . Blue: the total of events; red: accepted events. Right-hand side: the geometrical acceptance as function of  $x_\pi$ .

The target Bjorken  $x$  is studied following the same procedure. The plot shown in Fig. 13(b), implies that the higher values of target Bjorken  $x$  are not accepted. The plot 13(b) is identical to the one made in Ref. [4].

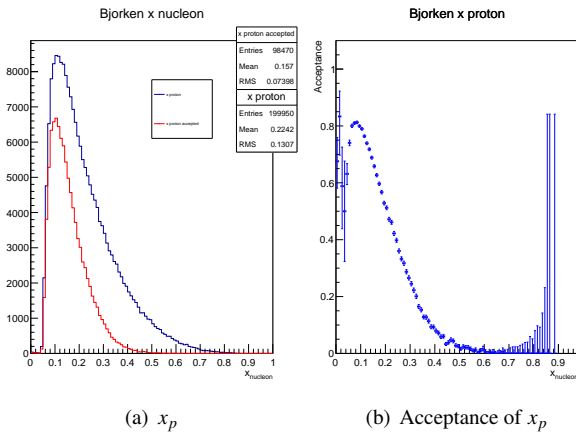


**Figure 13.** The target proton Bjorken  $x$ . Blue: the total of events; red: accepted events. Right-hand side: the geometrical acceptance as function of  $x_p$ .

### 3.5.3 Phase Space

Fig. 14 relates the Bjorken  $x$  of the beam ( $x$ -axis) with the target one ( $y$ -axis), illustrating the phase space of the proposed measurement.

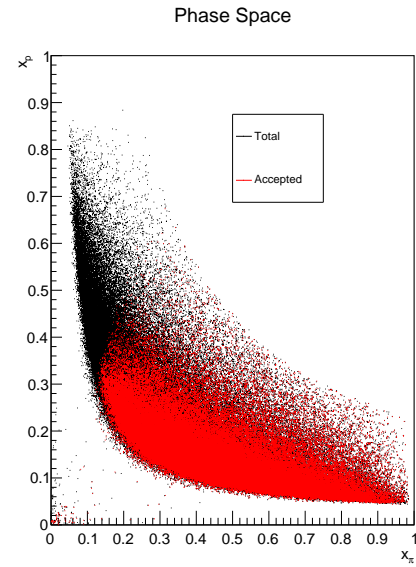


**Figure 14.** Phase space in  $x_p$  vs  $x_\pi$ . Black: the total of events; red: accepted events.

Just as shown before, this plot also acknowledges that the lower values of the  $x_\pi$  will not be accepted by the detectors, which corresponds to higher values for the  $x_p$ .

### 3.5.4 Feynman $x$

In Fig. 15(a), it is visible that with these cuts in the muon polar angle, the accepted events will be those with higher Feynman  $x$ . Basically only events with  $x_F > -0.2$  are accepted, i.e. events in the forward region.

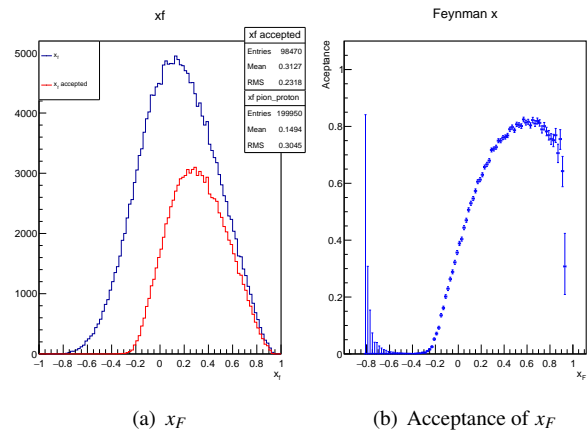


**Figure 15.** The Feynman  $x$ . Blue: the total of events; red: accepted events. Right-hand side: the geometrical acceptance as function of  $x_F$ .

The plot 15(b) shows the acceptance as a function of the Feynman  $x$ . It is nearly identical to the one presented in Ref. [4].

## 4 Conclusions

The PYTHIA simulation made allowed to evaluate some of the features of the Drell-Yan process.

First, the final state particle species and their momenta were studied. This type of simulation allows to optimise the detectors used, since they will be affected by the passage of these particles. Namely, it highlights the need for a hadron absorber in between the target and spectrometer, in order to avoid flooding the detectors with uninteresting particles.

The case where the beam particle is misidentified by another particle was studied, in order to analyze how the misidentification would change the DY kinematic variables.

It was also simulated the acceptance of the detectors, applying cuts in the muons polar angle. Even though this was used, this is still far from a real experiment, since here the target had no extension, and the detectors were not simulated.

The next steps would be to use a detector simulation pack-

age that allows to mimic the target and the detectors and takes that into account in the simulations made.

## 5 Acknowledgements

I would like to express gratitude to my supervisor, Catarina. I'm very grateful for all the guidance, attention and continuous support.

## References

- [1] B. Adams et al., CERN-SPSC-2019-022 (SPSC-P-360) (2019)
- [2] M. Aghasyan et al. (COMPASS Collaboration), *Phys. Rev. Lett.* **119**, 112002 (2017)
- [3] I.R. Kenyon, *Reports on Progress in Physics* **45**, 1261 (1982)
- [4] F. Gautheron et al. (COMPASS), CERN-SPSC-2010-014, SPSC-P-340 (2010)